

# The $L_X$ – $M$ Relation of Clusters of Galaxies

E. S. Rykoff,<sup>1</sup> A. E. Evrard,<sup>2 3 4</sup> T. A. McKay,<sup>2 3 4</sup> M. R. Becker,<sup>2 5</sup> D. E. Johnston,<sup>6</sup> B. P. Koester,<sup>7 8</sup> B. Nord,<sup>2</sup> E. Rozo,<sup>9</sup> E. S. Sheldon,<sup>10</sup> R. Stanek,<sup>3</sup> R. H. Wechsler<sup>11</sup>

<sup>1</sup> TABASGO Fellow, Physics Department, University of California at Santa Barbara, 2233B Broida Hall, Santa Barbara, CA 93106

<sup>2</sup> Physics Department, University of Michigan, Ann Arbor, MI 48109

<sup>3</sup> Astronomy Department, University of Michigan, Ann Arbor, MI 48109

<sup>4</sup> Michigan Center for Theoretical Physics, Ann Arbor, MI 48109

<sup>5</sup> Department of Physics, The University of Chicago, Chicago, IL 60637

<sup>6</sup> Jet Propulsion Laboratory, 4800 Oak Grove Drive, Pasadena, CA 91109

<sup>7</sup> Department of Astronomy and Astrophysics, The University of Chicago, Chicago, IL 60637

<sup>8</sup> Kavli Institute for Cosmological Physics, The University of Chicago, Chicago, IL 60637

<sup>9</sup> CCAPP Fellow, The Ohio State University, Columbus, OH 43210

<sup>10</sup> Center for Cosmology and Particle Physics, Physics Department, New York University, New York, NY 10003

<sup>11</sup> KIPAC, Physics Dept. and SLAC, Stanford University, Stanford, CA 94305

arXiv:0802.1069v1 [astro-ph] 7 Feb 2008

Draft: February 7, 2007

## ABSTRACT

We present a new measurement of the scaling relation between X-ray luminosity and total mass for 17,000 galaxy clusters in the maxBCG cluster sample. Stacking sub-samples within fixed ranges of optical richness,  $N_{200}$ , we measure the mean 0.1–2.4 keV X-ray luminosity,  $\langle L_X \rangle$ , from the *ROSAT* All-Sky Survey. The mean mass,  $\langle M_{200} \rangle$ , is measured from weak gravitational lensing of SDSS background galaxies (Johnston et al. 2007). For  $9 \leq N_{200} < 200$ , the data are well fit by a power-law,  $\langle L_X \rangle / 10^{42} h^{-2} \text{ erg s}^{-1} = (12.6_{-1.3}^{+1.4} \text{ (stat)} \pm 1.6 \text{ (sys)}) (\langle M_{200} \rangle / 10^{14} h^{-1} M_\odot)^{1.65 \pm 0.13}$ . The slope agrees to within 10% with previous estimates based on X-ray selected catalogs, implying that the covariance in  $L_X$  and  $N_{200}$  at fixed halo mass is not large. The luminosity intercept is 30%, or  $2.5\sigma$ , lower than that of Reiprich & Böhringer (2002), who applied a hydrostatic assumption to an X-ray flux-limited sample. This difference could arise from a combination of Malmquist bias and/or systematic error in hydrostatic mass estimates, both of which are expected. The intercept agrees with that derived by Stanek et al. (2006) using a model for the statistical correspondence between clusters and halos in a WMAP3 cosmology with power spectrum normalization  $\sigma_8 = 0.85$ . Similar exercises applied to future data sets will allow constraints on the covariance among optical and hot gas properties of clusters at fixed mass.

**Key words:** clusters: general – clusters: ICM – X-rays: clusters – clusters: calibration

## 1 INTRODUCTION

Bulk properties of galaxy clusters, such as galaxy richness and velocity dispersion, X-ray temperature and luminosity, mean weak gravitational lensing shear and X-ray hydrostatic mass, display strong internal correlations (for reviews, see Rosati et al. 2002; Voit 2005). Although these correlations are anticipated by dimensional arguments — the “bigger things are bigger in all measures” perspective — detailed theoretical expectations are complicated by baryon evolution uncertainties. Even with some baryon model prescribed, the stochastic nature of the halo evolution in a hierarchical clustering framework will impose variance about the mean

behavior, the scale of which is likely to be sensitive to the baryon prescription.

Improved understanding of cluster scaling relations is desirable on both astrophysical and cosmological grounds. Better astrophysical models of galaxy and hot gas evolution in halos will improve constraints on cosmological parameters obtained from studies of cluster samples (e.g. Vikhlinin et al. 2006; Rozo et al. 2007; Mantz et al. 2007).

The relation between X-ray luminosity  $L_X$  and halo mass  $M$  is a diagnostic of the halo baryon fraction and the entropy structure of the intracluster gas. From X-ray data alone, constraints on the  $L_X$ – $M$  relation have been obtained using either direct or statistical arguments. The direct approach assumes that the intracluster gas is in hydrostatic

equilibrium, so that observations of the X-ray surface brightness, which provides  $L_X$ , and the X-ray temperature profile can be combined to estimate thermal pressure gradients and, hence, cluster binding masses. Reiprich & Böhringer (2002, hereafter RB02) measured the  $L_X$ – $M$  relation in this manner for the X-ray flux limited HIFLUGCS sample of roughly 100 clusters (Finoguenov et al. 2001). The statistical approach, on the other hand, assumes a form for the likelihood,  $P(L_X|M, z)$ , which is convolved with the space density of halos in a given cosmology to predict cluster counts as a function of X-ray flux and redshift. This approach was applied by Stanek et al. (2006, hereafter S06) to the flux-limited REFLEX survey (Böhringer et al. 2004) using halo space densities calibrated for a  $\Lambda$ CDM cosmology (Jenkins et al. 2001; Evrard et al. 2002).

A third approach to the  $L_X$ – $M$  relation employs weak gravitational lensing mass estimates derived from shear patterns of background galaxies in deep optical imaging of cluster fields. Recently, Bardeau et al. (2007) and Hoekstra (2007) have performed such analysis of 11 and 20 clusters, respectively, at redshifts near  $z \sim 0.25$ . These studies provide a powerful cross check between the two methods, but provide a weaker constraint on the mass scaling as they focus on the X-ray luminous tail of the cluster population.

In this paper, we extend the dynamic range of the third approach using a large, uniform sample. We present the  $L_X$ – $M$  relation derived from  $\sim 17,000$  optically selected galaxy clusters in the maxBCG catalog (Koester et al. 2007b). Binning clusters by optical richness,  $N_{200}$ , we measure the mean X-ray luminosity,  $\bar{L}_X \equiv \langle L_X | N_{200} \rangle$ , using data from the *ROSAT* All-Sky Survey (RASS: Voges 1999). Details of the method are described in Rykoff et al. (2007, henceforth R07). The mean mass,  $\bar{M}_{200} \equiv \langle M_{200} | N_{200} \rangle^1$  of each bin is measured from analysis of the stacked weak gravitational lensing signal from SDSS galaxy images. Measurements of the shear are presented in Sheldon et al. (2007), and masses are derived by Johnston et al. (2007).

We begin with a brief description of the input data and the methods. We then present measurements of  $\bar{L}_X$  and  $\bar{M}_{200}$  for richness-binned maxBCG clusters, and compare the resultant scaling relation to the relations found by applying direct or statistical arguments to X-ray flux-limited samples. Throughout the paper, we assume a flat,  $\Lambda$ CDM cosmology with  $H_0 = 100 h \text{ km s}^{-1}$  and  $\Omega_m = 1 - \Omega_\Lambda = 0.3$ . In addition, our measurements are quoted at  $z = 0.25$ , close to the median redshift of the cluster catalog. Following R07, the X-ray luminosities are measured in the 0.1–2.4 keV observer frame, and  $k$ -corrected to rest frame 0.1–2.4 keV at  $z = 0.25$ .

## 2 INPUT DATA

Input data for this study comes from two large area surveys, the Sloan Digital Sky Survey (SDSS: York 2000) and RASS. SDSS imaging data are used to select the clusters and to measure the weak lensing shear around their centers. RASS data provide 0.1–2.4 keV X-ray luminosities,  $L_X$ , measured

<sup>1</sup> Here,  $M_{200}$  is the mass within a sphere of radius  $r_{200}$  that encompasses a mean density of  $200\rho_c(z)$ , with  $\rho_c$  the critical density.

within  $r_{200}$ . Here, we briefly describe the maxBCG cluster catalog, binning strategies, and our methods for calculating mean mass and X-ray luminosity.

### 2.1 maxBCG Catalog

The maxBCG cluster catalog provides sky locations, redshift estimates, and richness values for the cluster sample we employ. Details of the selection algorithm and catalog properties are published elsewhere (Koester et al. 2007a,b). In brief, maxBCG selection relies on the observation that the galaxy population of rich clusters is dominated by bright, red galaxies clustered tightly in color (the E/S0 ridgeline). Since these galaxies have old, passively evolving stellar populations, their  $g - r$  color closely reflects their redshift. The brightest such red galaxy, typically located at the peak of galaxy density, defines the cluster center.

The maxBCG catalog is approximately volume limited in the redshift range  $0.1 \leq z \leq 0.3$ , with very accurate photometric redshifts ( $\delta z \sim 0.01$ ). Studies of the maxBCG algorithm applied to mock SDSS catalogs indicate that the completeness and purity are very high, above 90% (Koester et al. 2007b; Rozo et al. 2007). The maxBCG catalog has been used to investigate the scaling of galaxy velocity dispersion with cluster richness (Becker et al. 2007) and to derive constraints on the power spectrum normalization,  $\sigma_8$ , from cluster number counts (Rozo et al. 2007).

The primary richness estimator used here is  $N_{200}$ , defined as the number of E/S0 ridgeline cluster members brighter than  $0.4 L_*$  (in  $i$ -band) found within  $r_{200}^N$  of the cluster center (Hansen et al. 2005). As a cross-check, we also bin the sample using a secondary richness estimator,  $L_{200}$ , the total  $k$ -corrected  $i$ -band luminosity of the cluster members. We note that  $N_{200}$  and  $L_{200}$  are strongly correlated, especially for the richer clusters. We use six richness bins with  $N_{200} \geq 9$ , described in Table 1, based on those used in the weak lensing analysis of Sheldon et al. (2007). The total number of clusters is 17335.

### 2.2 Measuring $\bar{L}_X$

We measure the mean 0.1–2.4 keV X-ray luminosity,  $\bar{L}_X$ , of the clusters in each bin by stacking photons from RASS. The typical RASS exposure time for maxBCG clusters is  $\sim 400$  s, too short to allow significant detections for all but the brightest individual clusters. By binning on  $N_{200}$  or  $L_{200}$  we can take advantage of the large number of maxBCG clusters. The stacking method is described in detail in R07, but there are a few differences in the analysis for this letter which we highlight here.

We stack all the photons in a scaled aperture from clusters in a given richness or optical luminosity bin, treating the brightest cluster galaxy selected by the maxBCG algorithm as the center of each cluster. In R07 we show that this assumption for centering does not introduce a significant bias in the calculation of  $\bar{L}_X$ . For consistency with the cluster mass calculations in Johnston et al. (2007), we scale all radii and luminosities to  $z = 0.25$ . This scale redshift is slightly larger than used in R07, but does not significantly change  $\bar{L}_X$ . After building scaled photon maps, we construct images, radial profiles, and spectra, and calculate an unabsorbed, rest-frame mean luminosity,  $\bar{L}_X$ , for each bin.

**Table 1.**  $\langle L_X | N_{200} \rangle$  and  $\langle M_{200} | N_{200} \rangle$ 

$N_{200}$ Range	$r_{200}$ ( $h^{-1}$ Mpc)	$\bar{L}_X$ [0.1 – 2.4 keV] ( $10^{42} h^{-2} \text{ erg s}^{-1}$ )	$\bar{M}_{200}$ ( $10^{14} h^{-1} M_\odot$ )
9 – 11	0.49	$2.72 \pm 0.35$	$0.441 \pm 0.080$
12 – 17	0.55	$5.65 \pm 0.37$	$0.600 \pm 0.085$
18 – 25	0.64	$12.8 \pm 0.98$	$0.96 \pm 0.13$
26 – 40	0.77	$30.6 \pm 2.3$	$1.68 \pm 0.23$
41 – 70	0.90	$56.7 \pm 4.5$	$2.52 \pm 0.36$
71 – 188	1.20	$209 \pm 31$	$5.69 \pm 0.88$

The X-ray luminosities are measured within scaled apertures,  $r_{200}$ , determined from the weak lensing mass profiles described in § 2.3. These radii are smaller, by  $\sim 50\%$  on average, than  $r_{200}^N$ , the optical richness based estimates derived in Hansen et al. (2005) and used in R07. We note that the richness based radial scale,  $r_{200}^N$ , defines the order parameters,  $N_{200}$  and  $L_{200}$ , in the maxBCG catalog. However, our mass and luminosity estimates in this letter consistently employ  $r_{200}$  derived from the weak lensing profiles. Since  $L_X$  is proportional to the gas density squared, most of the flux originates near the dense core and the effect of this rescaling is modest. Decreasing the aperture from  $r_{200}^N$  to  $r_{200}$  reduces the measured values of  $\bar{L}_X$  by  $\sim 10\% – 15\%$ .

The best-fit spectral temperatures are used to  $k$ -correct the observed 0.1–2.4 keV emission to the rest frame at  $z = 0.25$ . Values for the case of  $N_{200}$  binning are listed in Table 1. As shown in R07, the data are well fit by a power law form,

$$\langle L_X | N_{200} \rangle = (42.1 \pm 1.7) (N_{200}/40)^{1.88 \pm 0.06} \times 10^{42} \text{ erg s}^{-1}. \quad (1)$$

### 2.3 Measuring $\bar{M}_{200}$

The mean projected surface density contrast, measured from the shear of faint background galaxies as a function of projected distance from the cluster center was calculated by Sheldon et al. (2007) for the binned samples employed in this letter. However, as maxBCG clusters are not guaranteed to be centered on the mass density peaks of dark halos, Johnston et al. (2007) calculate mean cluster masses using a mass model that incorporates a degree of halo mis-centering.

Specifically, the projected surface density contrast in a given bin is modeled as a sum of four components: i) a small scale component from the stellar mass of the central galaxy; ii) a mean NFW (Navarro et al. 1997) halo; iii) a large-scale component arising from the clustering of halos (the two-halo term); and iv) a correction for the subset of clusters with BCG centers offset from halo centers. The mean halo mass,  $\bar{M}_{200}$ , and its uncertainty are obtained by marginalizing over the posterior probability distribution using a Markov Chain Monte Carlo (MCMC) method. The resultant masses, listed in Table 1, scale as a power-law in richness,

$$\langle M_{200} | N_{200} \rangle = (2.1 \pm 0.3) (N_{200}/40)^{1.28 \pm 0.04} \times 10^{14} M_\odot, \quad (2)$$

where the error in the intercept is dominated by systematic uncertainties in the photometric redshifts of background galaxies, in the absolute shear calibration, and in the calibration of the mis-centering model.

### 3 THE $\bar{L}_X$ – $\bar{M}_{200}$ RELATION

In Fig. 1 we plot the mean luminosities and lensing masses using binning in  $N_{200}$  (Table 1, filled symbols) or in  $L_{200}$  (open symbols). The two binning choices offer consistent results. The gray band shows the best-fit maxBCG–RASS relation ( $\pm 1\sigma$ ) from  $N_{200}$  binning,

$$\langle L_X | N_{200} \rangle = 12.6^{+1.4}_{-1.3} \left( \frac{\langle M_{200} | N_{200} \rangle}{10^{14} h^{-1} M_\odot} \right)^{1.65 \pm 0.13} 10^{42} \text{ erg s}^{-1}. \quad (3)$$

We estimate an additional systematic error of  $\pm 1.6$  in normalization due to the mass scale uncertainties described in the previous section. The two additional lines show results from X-ray flux-limited cluster samples. The RB02 result using hydrostatic mass estimates is the dashed line and the S06 result using a statistical halo model is the dot-dashed. The S06 result depends on the assumed cosmology, and they employ a  $\Lambda$ CDM model with  $\Omega_m = 0.24$ , spectral index  $n_s = 1$ , and power spectrum normalization  $\sigma_8 = 0.85$ . For this model, the inferred scatter in mass at fixed  $L_X$  is  $\sigma_{\ln M | L} = 0.25$ , equivalent to luminosity scatter,  $\sigma_{\ln L | M} = 0.40$ . To properly compare with the algebraic mean luminosity of maxBCG–RASS, we adjust the published normalizations of RB02 and S06 by a factor  $\exp(0.5\sigma_{\ln L | M}^2)$ , resulting in an  $\sim 8\%$  increase in luminosity at fixed mass.

The slope of the maxBCG–RASS relation,  $1.65 \pm 0.13$ , agrees well with the values found previously. The RB02 result,  $1.50 \pm 0.08$ , is somewhat shallower, but not significantly so, and the S06 result,  $1.59 \pm 0.05$ , is consistent with the present determination. The normalization of the maxBCG–RASS relation is consistent with the S06 results, with the RB02 masses lying  $2 – 3\sigma$  low. Further discussion of these results is in § 4 below.

The maxBCG–RASS normalization can be compared with recent lensing results published for small samples of massive clusters at  $z \sim 0.25$ . Bardeau et al. (2007) and Hoekstra (2007) performed weak lensing analyses of 11 and 20, respectively, individual clusters. Both studies focus on selected high luminosity clusters, with  $L_X > 10^{44} h^{-2} \text{ erg s}^{-1}$ , at redshifts near the median of the maxBCG catalog. Both papers find a correlation between  $L_X$  and  $M_{200}$ , but with noisy lensing mass estimates. As each study employs a different convention for  $L_X$ , we have recalculated  $L_X$  for these clusters using RASS photon data (see § 4.1 in R07). Fixing the slope at 1.6, we compute the normalization of  $L_X / 10^{44} h^{-2} \text{ erg s}^{-1}$  at  $10^{15} h^{-1} M_\odot$ , finding  $11 \pm 2$  and  $5.0 \pm 0.6$  for the Bardeau et al. (2007) and Hoekstra (2007) clusters, respectively. At this high mass scale, the Hoekstra (2007) normalization is consistent with our value, while the Bardeau et al. (2007) is  $\sim 2\sigma$  larger. A full accounting for this discrepancy is beyond the scope of this work.

### 4 DISCUSSION

The good level of agreement displayed in Fig. 1 among three independent approaches to determining the  $L_X$ – $M$  relation indicates that optical and X-ray selection methods are finding similar populations of massive halos. Furthermore, the maxBCG–RASS result extends to a lower mass scale than is probed by RB02 and S06. In this section, we point out

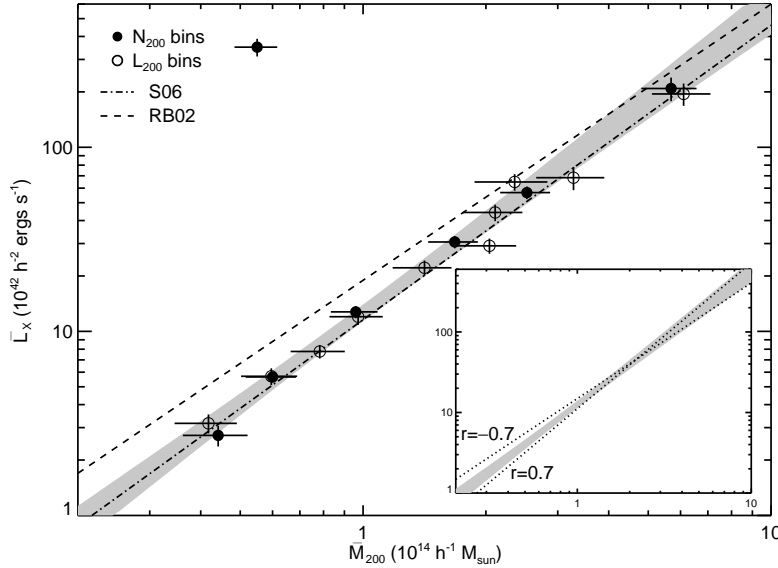


**Figure 1.** Points show maxBCG–RASS (algebraic) mean  $L_X$  and  $M_{200}$  values found by binning on  $N_{200}$  (solid circles) or  $L_{200}$  (empty circles). The dark gray band represents the  $\pm 1\sigma$  contours on the best fit relation using the  $N_{200}$  bins. The best-fit relation using  $L_{200}$  bins is fully consistent. The dot-dashed line shows the S06 relation with  $\Omega_m = 0.24$ ,  $\sigma_8 = 0.85$ , while the dashed line shows the RB02 result based on hydrostatic masses. The error bar in the legend shows the typical  $1\sigma$  systematic error in the SDSS lensing masses, representing an overall shift in normalization that is possible in the maxBCG–RASS relation. The inset plot indicates the effects on the slope due to covariance between  $L_X$  and  $N_{200}$  at fixed mass ( $r$ ), as described in § 4. If  $L_X$  and  $N_{200}$  at fixed mass are correlated ( $r = 0.7$ ), this will bias the slope steeper, and if they are anti-correlated, this will bias the slope shallower.

effects that could lead to differences among the three measurements. The discussion is aimed at raising issues to be addressed by more detailed analysis in future work.

Non-zero bias in hydrostatic mass estimates, displayed in early, low-resolution gas simulations (Evrard 1990), is a possible source of systematic error that would shift the RB02 result relative to the true relation. Recent studies using mock X-ray exposures of numerical simulations predict a systematic underestimate of binding mass at the level of  $-0.25$  in  $\ln M$  (Rasia et al. 2005; Nagai et al. 2007). Correcting the RB02 result by this amount would more closely align it with the maxBCG–RASS relation. Assuming the latter is an unbiased estimate of the underlying halo relation, the luminosity offset between the two relations measures the Malmquist bias arising from the X-ray flux limit of the HIFLUGCS sample used by RB02. Good agreement would signal a small bias, meaning small intrinsic scatter ( $\lesssim 10\%$ ) between luminosity and mass. Such small scatter is considered unlikely by the analysis of S06.

A separate argument can be made based on slope estimates. If hydrostatic mass estimates scale with true mass as  $\langle M_{\text{est}} \rangle \propto M_{\text{true}}^{1+\epsilon}$ , then one would expect the RB02 slope to differ by  $1.5\epsilon$  from the maxBCG–RASS value. The measured slope difference,  $0.15 \pm 0.15$ , implies  $\epsilon = 0.1 \pm 0.1$ . Strongly mass dependent hydrostatic biases are therefore ruled out.

One could shift the RB02 result to higher masses without requiring a major reduction in scatter,  $\sigma_{\ln M|L}$ , as constrained in S06. This would require shifting the S06 result by modifying the assumed cosmology. The luminosity normalization is sensitive to power spectrum normalization,  $L_X \sim \sigma_8^{-4}$ , so raising  $\sigma_8$  to 0.95 would shift the S06 result to lower  $L_X$  and preserve the current level of Malmquist-bias

for the RB02 result. However, this adjustment would offset the S06 and maxBCG–RASS relations at the  $2\sigma$  level.

Since it is binned by richness, the maxBCG–RASS result is sensitive to covariance among  $L_X$  and  $N_{200}$  at fixed  $M_{200}$ . Simulations suggest mild anti-correlation, as at fixed mass high concentration halos have higher  $L_X$  but fewer galaxies (Wechsler et al. 2006). As an illustration of the effect of covariance, consider the case of a bivariate, log-normal distribution for  $L_X$  and  $N_{200}$  with constant covariance. The off-diagonal term can be characterized by the correlation coefficient,  $r \equiv \langle \delta_{\ln L} \delta_{\ln N} \rangle$ , where  $\delta_{\ln X} = (\ln X - \ln \bar{X}) / \sigma_{\ln X}$  are the normalized deviations from the mean relation.

Consider a mass function that is a local power-law,  $dn/d\ln M \sim M^{-\alpha} = e^{-\alpha\mu}$ , where  $\mu \equiv \ln M$ . Convolving this function with the bivariate log-normal, and using Bayes' theorem, allows one to write the conditional likelihood  $P(\ell, \mu|\nu)$ , where  $\ell \equiv \ln L_X$  and  $\nu \equiv \ln N_{200}$ . The result is a bivariate Gaussian with mean mass  $\bar{\mu}(\nu) = \bar{\mu}_0(\nu) - \alpha\sigma_{\mu|\nu}^2$ , with  $\bar{\mu}_0(\nu)$  the inverse of the input mean richness–mass relation and  $\sigma_{\mu|\nu}$  the scatter in mass at fixed richness. The X-ray luminosity at fixed optical richness is distributed in a log-normal manner with mean

$$\bar{\ell}(\nu) = p \cdot (\bar{\mu}(\nu) + \alpha r \sigma_{\mu|\nu} \sigma_{\mu|\ell}), \quad (4)$$

and variance

$$\sigma_{\ell|\nu}^2 = p^2 \cdot (\sigma_{\mu|\nu}^2 + \sigma_{\mu|\ell}^2 - 2r\sigma_{\mu|\nu}\sigma_{\mu|\ell}), \quad (5)$$

where  $p$  is the slope of the halo  $L_X - M_{200}$  relation.

When  $L_X$  and  $N_{200}$  are independent ( $r = 0$ ), the mean luminosity reflects that of the mean mass selected by the richness cut. When  $r \neq 0$ , the mean is shifted by an amount that scales linearly with the mass function slope  $\alpha$ . If the

scatter is constant, then this shift affects all  $N_{200}$ -binned points equally, and the slope of the richness-binned  $L_X$ – $M_{200}$  relation will be unbiased,  $d\bar{\ell}(\nu)/d\bar{\mu}(\nu) = p$ . However, in cold dark matter models, the slope  $\alpha$  runs with mass, and this running can induce a change in slope at the level  $\Delta p/p = r\sigma_{\mu|\nu}\sigma_{\mu|\ell}(d\alpha(\mu)/d\mu)$ .

The inset of Fig. 1 explicitly demonstrates this effect for the case  $p = 1.6$ ,  $\sigma_{\mu|\ell} = 0.25$  and  $\sigma_{\mu|\nu} = 0.5$ . We use a discrete set of halos from the Hubble Volume simulation (Evrard et al. 2002) that define a mass function which is not a power-law (Jenkins et al. 2001). To each halo, we assign richness and luminosity using a constant log-normal covariance, then bin the sample on optical richness and compute mean luminosities and masses for each bin. Imposing a correlation coefficient  $r = \pm 0.7$  tilts the richness-binned  $L_X$ – $M_{200}$  slope by  $\sim 0.2$ , or roughly  $1.5\sigma$  given the error in Eq. (3).

As discussed in Nord et al. (2007), covariance can both tilt the scaling relation and modify the scatter. The second observable quantity affected by  $r$  is the variance in  $L_X$  at fixed richness  $N_{200}$ , Eq. (5). This scatter was constrained in R07 to be  $\sigma_{\ell|\nu} = 0.86 \pm 0.03$ . In our model, it takes on values of 1.1, 0.90, and 0.72 for  $r = -0.7, 0$ , and 0.7, respectively. We stress that these values are sensitive to the assumed degree of mass scatter at fixed  $N_{200}$ . Our assumed value of 0.5 is smaller than that inferred by the spread in galaxy velocity dispersions at fixed richness (Becker et al. 2007) and employed by Johnston et al. (2007) in the lensing analysis. Using this larger scatter would result in  $\sigma_{\ell|\nu} > 1$  for all  $r \in [-1, 1]$ . If the R07 measurement of  $\sigma_{\ell|\nu} \lesssim 0.9$  is correct, then either the Becker et al. (2007) scatter is an overestimate or the simple log-normal model employed here is insufficient.

Improved understanding of the variance is clearly desired. Constraints on  $\sigma_{\ell|\nu}$  can be obtained by individual X-ray follow-up observations of richness-selected maxBCG subsamples. Such data can also generate hydrostatic mass estimates, enabling constraints on the mass scatter  $\sigma_{\mu|\nu}$ . Such a study would begin to test all the elements of the full covariance  $P(\ell, \nu|\mu)$  used to describe the underlying massive halo population.

## 5 SUMMARY

In this letter, we present a new measurement of the scaling between X-ray luminosity and mass using  $\sim 17,000$  optically-selected clusters of galaxies. X-ray luminosities are derived from RASS photon maps, while masses are determined independently through modeling of the mean cluster lensing profiles. Binning clusters by optical richness, we find that the mean  $L_X$  and  $M_{200}$  values follow a power-law relation with slope  $1.65 \pm 0.13$ . The consistency in slope with previous studies, including those based on hydrostatic mass estimates, confirms that the optically-selected maxBCG catalog selects a population of massive halos similar to those of X-ray samples. The consistency implies that systematic errors in hydrostatic mass are not strongly scale-dependent. Furthermore, we demonstrate how the slope can be affected by covariance in  $L_X$  and  $N_{200}$  at fixed mass, and show that this covariance is not large.

Follow-up X-ray observations of  $N_{200}$  selected subsam-

ples would provide key information on the covariance, as expressed in Eq. (5). Data from future deep surveys, selected via optical, X-ray and Sunyaev-Zel'dovich signatures, will provide a much richer environment for addressing the complex interplay between cosmology and covariant scaling relations.

## Acknowledgements

ESR and TAM are pleased to acknowledge financial support from NSF AST-0206277 and AST-0407061, and the hospitality of the Michigan Center for Theoretical Physics. ESR also thanks the TABASGO foundation. AEE acknowledges support from NSF AST-0708150.

## REFERENCES

Bardeau S., Soucail G., Kneib J.-P., Czoske O., Ebeling H., Hudelot P., Smail I., Smith G. P., 2007, A&A, 470, 449  
 Becker M. R., et al., 2007, ApJ, 669, 905  
 Böhringer H., et al., 2004, A&A, 425, 367  
 Ebeling H., Voges W., Böhringer H., Edge A. C., Huchra J. P., Briel U. G., 1996, MNRAS, 281, 799  
 Evrard A. E., 1990, ApJ, 363, 349  
 Evrard A. E., et al., 2002, ApJ, 573, 7  
 Finoguenov A., Reiprich T. H., Böhringer H., 2001, A&A, 368, 749  
 Gioia I. M., Maccacaro T., Schild R. E., Wolter A., Stocke J. T., Morris S. L., Henry J. P., 1990, ApJS, 72, 567  
 Hansen S. M., McKay T. A., Wechsler R. H., Annis J., Sheldon E. S., Kimball A., 2005, ApJ, 633, 122  
 Hoekstra H., 2007, astro-ph/0705.0358  
 Jenkins A., Frenk C. S., White S. D. M., Colberg J. M., Cole S., Evrard A. E., Couchman H. M. P., Yoshida N., 2001, MNRAS, 321, 372  
 Johnston D. E., et al., 2007, astro-ph/0709.1159  
 Koester B. P., et al., 2007, ApJ, 660, 221  
 Koester B. P., et al., 2007, ApJ, 660, 239  
 Mantz A., Allen S. W., Ebeling H., Rapetti D., 2007, astro-ph/0709.4294  
 Nagai D., Vikhlinin A., Kravtsov A. V., 2007, ApJ, 655, 98  
 Navarro J. F., Frenk C. S., White S. D. M., 1997, ApJ, 490, 493+  
 Nord B., Stanek R., Rasia E., Evrard A. E., 2007, astro-ph/0706.2189  
 Rasia E., Mazzotta P., Borgani S., Moscardini L., Dolag K., Tormen G., Diaferio A., Murante G., 2005, ApJL, 618, L1  
 Reiprich T. H., Böhringer H., 2002, ApJ, 567, 716  
 Rosati P., Borgani S., Norman C., 2002, ARA&A, 40, 539  
 Rozo E., et al., 2007, astro-ph/0703571  
 Rykoff E. S., et al., 2007, astro-ph/0709.1158  
 Sheldon E. S., et al., 2007, astro-ph/0709.1153  
 Stanek R., Evrard A. E., Böhringer H., Schuecker P., Nord B., 2006, ApJ, 648, 956  
 Vikhlinin A., Kravtsov A., Forman W., Jones C., Markevitch M., Murray S. S., Van Speybroeck L., 2006, ApJ, 640, 691  
 Voges W., et al., 1999, A&A, 349, 389  
 Voit G. M., 2005, Reviews of Modern Physics, 77, 207  
 Wechsler R. H., Zentner A. R., Bullock J. S., Kravtsov A. V., Allgood B., 2006, ApJ, 652, 71  
 York D. G., et al., 2000, AJ, 120, 1579